SCIENCE CHINA
Technological Sciences

•Article•

April 2023 Vol.66 No.4: 1038–1049
https://doi.org/10.1007/s11431-022-2219-9

Thermoelastic rotating contact of an FGM coating with temperature-dependent and arbitrary varying properties

ZHOU JiaLin[1], SHEN Fei[1], LIU Jing[2], EL-BORGI Sami[3] & KE LiaoLiang[1*]

[1] *Department of Mechanics, School of Mechanical Engineering, Tianjin University, Tianjin 300350, China;*
[2] *College of Engineering, Huazhong Agricultural University, Wuhan 430070, China;*
[3] *Mechanical Engineering Program, Engineering Building, Texas A&M University at Qatar, Education City, Doha, P.O. Box 23874, Qatar*

Received August 8, 2022; accepted September 22, 2022; published online March 14, 2023

This paper investigates the frictional thermoelastic contact of a rigid spherical punch and functionally graded material (FGM) coated half-space with arbitrarily varying material properties. These material parameters include the elastic modulus, Poisson's ratio, heat conduction parameter, and thermal expansion coefficient. The material parameters of the FGM coating and half-space are assumed to be temperature dependent. The spherical punch is rotated in the FGM-coated half-space at a constant angular speed. The generated frictional heat is related to the friction coefficient, contact radius, angular velocity, and contact pressure. A theoretical formula for the thermoelastic rotating contact problem is established and solved using the finite element method. The main objective of this paper is to investigate the effects of temperature dependence, gradient index, friction coefficient, angular velocity, and gradient form on the surface temperature and stresses.

rotating punch, frictional heat, functionally graded materials, temperature dependence, arbitrary properties

Citation: Zhou J L, Shen F, Liu J, et al. Thermoelastic rotating contact of an FGM coating with temperature-dependent and arbitrary varying properties. Sci China Tech Sci, 2023, 66: 1038–1049, https://doi.org/10.1007/s11431-022-2219-9

1 Introduction

Many realistic contact problems involve frictional heat, such as the brake systems of high-speed trains, contacts between pantographs and power grids, and friction stir welding. Contact with frictional heat may cause thermoelastic deformation and material wear of the contact surface, which results in material damage or even catastrophic failure under long-term service. If the two contact bodies have different temperatures, the induced thermoelastic deformation affects the contact pressure distribution and contact radius. These changes also affect the boundary conditions of the heat conduction problem, resulting in thermomechanical coupling [1]. Functionally graded materials (FGMs) are inhomogeneous materials with properties that vary gradually along a given spatial direction. Owing to the gradient change in material properties, the local stress concentration is reduced, the material resistance to contact deformation and damage is improved, and as a result, the contact components can complete their functional tasks under different conditions [2–4]. Many experimental and theoretical studies have shown that using FGMs as coatings or transition layers can improve the surface performance and provide protection in harsh thermal and chemical environments [5–7].

Over the past two decades, many investigators have studied the elastic contact problem of FGMs or FGM coatings [8–15]. Guler and Erdogan [16,17] analyzed the contact problem of an FGM coating using a rigid punch. Ke and Wang [18] employed a multi-layered model and the transfer matrix method to investigate the contact problem of an FGM coating with arbitrary material properties. Liu et al. [19] used a layered model to analyze the axisymmetric frictionless

*Corresponding author (email: llke@tju.edu.cn)

© Science China Press 2023

contact between a punch and FGM coating. Dag et al. [20] obtained the numerical solution of a rigid punch and an FGM half-plane with a lateral gradient. This problem was also analyzed using the finite element method (FEM), and both the theoretical and FEM results were in good agreement. Çömez [21] considered a moving contact problem for a rigid cylindrical punch and an FGM layer of finite thickness. Chen et al. [22,23] studied the sliding contact problem between a rigid punch and an FGM half-plane with a gradient in two directions. El-Borgi et al. [24,25] discussed the frictional receding contact of an FGM coating and concluded that the non-uniform parameters of the coating affected the receding contact length. Aizikovich et al. [26,27] presented an analytical method for solving the elastic half-space with a graded coating.

The thermoelastic contact of FGMs with frictional heat generation has become an active research direction [28–35]. Choi and Paulino [36] first considered the thermoelastic contact problem between a rigid flat punch and a coating-graded interlayer-substrate system and converted this problem into a singular integral equation. Barik and Chaudhuri [37] studied the thermoelastic contact of an FGM cylindrical punch on an FGM half-space with exponential variation. Chen et al. [38,39] analyzed the sliding contact between a rigid punch and a finite FGM layer considering frictional heat. Liu et al. [40] solved the thermoelastic contact between a rigid punch and an FGM-coated half-plane with arbitrarily varying properties. They observed that changing the gradient form can improve the resistance to thermal contact damage. Balci et al. [41] investigated the sliding contact with frictional heat generation between a flat punch and an FGM-coated half-plane using commercial finite element software. Nili et al. [42,43] first studied the rolling thermoelastic contact problem of a rigid insulated roller and FGM-coated half-plane.

It is important to note that the studies mentioned above did not consider temperature-dependent material properties. Furthermore, for simplicity, the exponential function was mostly used to simulate the inhomogeneity of FGMs. In actual engineering applications, FGMs should be permitted to vary arbitrarily in a given spatial direction. To fill these gaps, this paper investigates the thermoelastic rotating contact between a spherical punch and an FGM-coated half-space with temperature-dependent material properties. The rotation of the spherical punch induces frictional heat between the punch and coating. The gradient form of the coating can be changed using arbitrary functions. The theoretical formula of the thermoelastic rotating contact problem is established and solved using the FEM. The effects of the temperature dependence, gradient index, friction coefficient, angular velocity, and gradient form on the surface temperature and stress are discussed.

The remainder of this paper is organized as follows. The considered problem and model description are presented in Sect. 2. The theoretical formulation of the thermoelastic rotating contact with the temperature dependence of the material properties is briefly summarized in Sect. 3. The finite element model is described in Sect. 4. Based on a detailed parametric study, the results are presented and discussed in Sect. 5. Finally, concluding remarks are presented in Sect. 6.

2 Model description

Figure 1 shows the axisymmetric frictional thermoelastic contact of a rotating rigid spherical punch on an FGM-coated half-space with arbitrary material properties. The material parameters of the FGM-coated half-space are dependent on the temperature. The thickness of the FGM coating is h. A concentrated normal force P is applied to the punch, which rotates at a constant angular speed ω on the FGM coating. The contact region is $0 \leqslant r \leqslant a$. Owing to the rotation of the punch, frictional heat is generated over the contact region, resulting in a temperature change in the FGM-coated half-space.

Material parameters with temperature dependence are considered for the FGM coating and the homogeneous half-space. The temperature-dependent material parameters can be expressed as [44]

$$B(T) = B_0\left(B_{-1}T^{-1} + 1 + B_1T + B_2T^2 + B_3T^3\right), \tag{1}$$

where $B(T)$ is the material parameter related to temperature T, such as the elastic modulus E, Poisson's ratio ν, thermal conductivity k, and thermal expansion coefficient α. B_0, B_{-1}, B_1, B_2, and B_3 are the coefficients, which can be obtained through experiments. The material parameters are assumed to be continuous at the interface $z = -h$.

For the FGM coating, all material properties are assumed to be temperature-dependent and vary along the z direction. These parameters are the elastic modulus, Poisson's ratio,

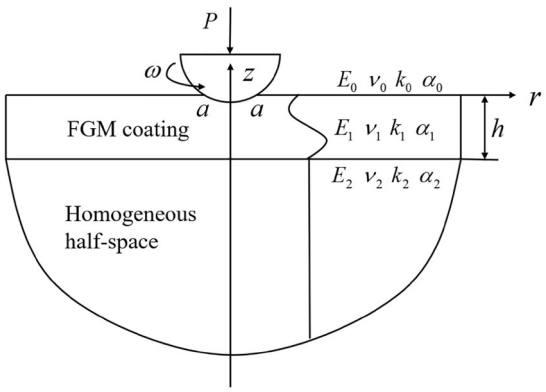

Figure 1 Schematic of the thermoelastic contact of a rigid spherical punch rotating on an FGM-coated half-space.

heat conduction parameter, and thermal expansion coefficient, and are denoted by $E_1(T, z)$, $v_1(T,z)$, $k_1(T, z)$, and $\alpha_1(T, z)$, respectively. Because this model can simulate FGMs with arbitrarily varying properties, four different gradient forms are discussed: the power-law form (case I), exponential form (case II), cosine form (case III), and sinusoidal form (case IV). Except for case II, it is difficult to provide an analytical solution for the mechanics problem of the FGM coatings described by the other three cases. Furthermore, the objective of selecting these cases is to discuss the effect of the gradient form on the thermoelastic contact behavior, which is important for coating design to resist thermoelastic contact damage.

The power-law form (case I) is given by

$$E_1(T, z) = E_0(T) + \left[E_2(T) - E_0(T)\right]|z / h|^n, \tag{2a}$$

$$v_1(T, z) = v_0(T) + \left[v_2(T) - v_0(T)\right]|z / h|^n, \tag{2b}$$

$$k_1(T, z) = k_0(T) + \left[k_2(T) - k_0(T)\right]|z / h|^n, \tag{2c}$$

$$\alpha_1(T, z) = \alpha_0(T) + \left[\alpha_2(T) - \alpha_0(T)\right]|z / h|^n, \tag{2d}$$

where n is the gradient index; the subscripts 0 and 2 are used to distinguish the material parameters at the upper and lower surface of the FGM coating, respectively. Note that the material parameters are continuous at the interface $z = -h$. Therefore, $E_2(T)$, $v_2(T)$, $k_2(T)$, and $\alpha_2(T)$ are also the parameters for the homogeneous half-space.

The exponential form (case II) is given by

$$E_1(T, z) = E_0(T)e^{\beta z},\ \beta = \log\left[E_0(T) / E_2(T)\right] / h, \tag{3a}$$

$$v_1(T, z) = v_0(T)e^{\psi z},\ \psi = \log\left[v_0(T) / v_2(T)\right] / h, \tag{3b}$$

$$k_1(T, z) = k_0(T)e^{\gamma z},\ \gamma = \log\left[k_0(T) / k_2(T)\right] / h, \tag{3c}$$

$$\alpha_1(T, z) = \alpha_0(T)e^{\varphi z},\ \varphi = \log\left[\alpha_0(T) / \alpha_2(T)\right] / h, \tag{3d}$$

where β, ψ, γ, and φ are the gradient indices.

The cosine form (case III) is given by

$$E_1(T, z) = \left[E_0(T) + E_2(T)\right] / 2 + \left[E_0(T) - E_2(T)\right]\cos(\pi z / h) / 2, \tag{4a}$$

$$v_1(T, z) = \left[v_0(T) + v_2(T)\right] / 2 + \left[v_0(T) - v_2(T)\right]\cos(\pi z / h) / 2, \tag{4b}$$

$$k_1(T, z) = \left[k_0(T) + k_2(T)\right] / 2 + \left[k_0(T) - k_2(T)\right]\cos(\pi z / h) / 2, \tag{4c}$$

$$\alpha_1(T, z) = \left[\alpha_0(T) + \alpha_2(T)\right] / 2 + \left[\alpha_0(T) - \alpha_2(T)\right]\cos(\pi z / h) / 2. \tag{4d}$$

Finally, the sinusoidal form (case IV) is given by

$$E_1(T, z) = E_0(T) + \left[E_0(T) - E_2(T)\right]\sin(\pi z / 2h), \tag{5a}$$

$$v_1(T, z) = v_0(T) + \left[v_0(T) - v_2(T)\right]\sin(\pi z / 2h), \tag{5b}$$

$$k_1(T, z) = k_0(T) + \left[k_0(T) - k_2(T)\right]\sin(\pi z / 2h), \tag{5c}$$

$$\alpha_1(T, z) = \alpha_0(T) + \left[\alpha_0(T) - \alpha_2(T)\right]\sin(\pi z / 2h). \tag{5d}$$

If all the heat generated by the rotating friction is transferred to the FGM-coated half-space, the heat flux density $Q(r)$ can be expressed as

$$Q(r) = f\omega r p(r),\ 0 \leqslant r \leqslant a, \tag{6}$$

where a denotes the contact radius, $p(r)$ denotes the contact pressure, and f denotes the friction coefficient.

3 Theoretical model with temperature-dependency

3.1 Temperature field

In this paper, the spherical punch is assumed to rotate at a constant angular speed on the FGM coating. The inertia effect can be ignored; therefore, the use of the steady-state heat conduction equation is reasonable for the thermoelastic rotating contact. Therefore, we obtain

$$\frac{1}{r}\frac{\partial}{\partial r}\left(k_i r\frac{\partial T_i}{\partial r}\right) + \frac{\partial}{\partial z}\left(k_i\frac{\partial T_i}{\partial z}\right) = 0, \tag{7}$$

where subscripts i = 1 and 2 refer to the FGM coating and homogeneous half-space, respectively; T_i is the temperature field; $k_1 = k_1(z, T_1)$ and $k_2 = k_2(T_2)$ are the heat conduction parameters for the FGM coating and half-space, respectively.

The thermal boundary conditions are given by

$$k_1\frac{\partial T_1(r,z)}{\partial z} = f\omega r p(r),\ 0 \leqslant r < a, \tag{8}$$

on the contact surface $z = 0$, and

$$k_1\frac{\partial T_1(r,z)}{\partial z} = k_2\frac{\partial T_2(r,z)}{\partial z}, \tag{9}$$

$$T_1(r,z) = T_2(r,z), \tag{10}$$

on the interface $z = -h$.

Note that the heat conduction eq. (7) is difficult to solve analytically because the material parameters are nonlinear functions of temperature. However, if the temperature dependence is neglected, eq. (7) can be solved to obtain a closed-form solution [45].

3.2 Stress field

The thermoelastic constitutive equations of the FGM coating and homogeneous half-space in the cylindrical coordinate system can be expressed as

$$\sigma_{rri}(r,z,T_i) = \left(\lambda_i + 2\mu_i\right)\frac{\partial u_i}{\partial r} + \lambda_i\left(\frac{u_i}{r} + \frac{\partial w_i}{\partial z}\right) - 3\alpha_i K_i T_i, \tag{11}$$

$$\sigma_{zz_i}(r,z,T_i) = (\lambda_i+2\mu_i)\frac{\partial w_i}{\partial z}+\lambda_i\left(\frac{u_i}{r}+\frac{\partial u_i}{\partial r}\right)-3\alpha_i K_i T_i, \tag{12}$$

$$\sigma_{\theta\theta i}(r,z,T_i) = (\lambda_i+2\mu_i)\frac{u_i}{r}+\lambda_i\left(\frac{\partial u_i}{\partial r}+\frac{\partial w_i}{\partial z}\right)-3\alpha_i K_i T_i, \tag{13}$$

$$\sigma_{rzi}(r,z,T_i) = \mu_i\left(\frac{\partial u_i}{\partial z}+\frac{\partial w_i}{\partial r}\right), \tag{14}$$

where $\lambda_i = v_i E_i/(1+v_i)(1-2v_i)$ and $\mu_i = E_i/2(1+v_i)$ are the Lamé constants, $K_i = E_i/3(1-2v_i)$ is the bulk modulus, u_i and w_i are displacements in the r and z directions, respectively. For the FGM coating, we have $\sigma_{rr1} = \sigma_{rr1}(r,z,T_1)$, $\sigma_{zz1} = \sigma_{zz1}(r,z,T_1)$, $\sigma_{\theta\theta1} = \sigma_{\theta\theta1}(r,z,T_1)$, $\lambda_1 = \lambda_1(z,T_1)$, $\mu_1 = \mu_1(z,T_1)$, $\alpha_1 = \alpha_1(z,T_1)$, and $K_1 = K_1(z,T_1)$. For the half-space, we have $\sigma_{rr2} = \sigma_{rr2}(r,z,T_2)$, $\sigma_{zz2} = \sigma_{zz2}(r,z,T_2)$, $\sigma_{\theta\theta2} = \sigma_{\theta\theta2}(r,z,T_2)$, $\lambda_2 = \lambda_2(T_2)$, $\mu_2 = \mu_2(T_2)$, $\alpha_2 = \alpha_2(T_2)$, and $K_2 = K_2(T_2)$.

The equilibrium equations are given by

$$\frac{\partial\sigma_{rri}}{\partial r}+\frac{\partial\sigma_{rzi}}{\partial z}+\frac{\sigma_{rri}-\sigma_{\theta\theta i}}{r} = 0, \tag{15}$$

$$\frac{\partial\sigma_{rzi}}{\partial r}+\frac{\partial\sigma_{zzi}}{\partial z}+\frac{\sigma_{rzi}}{r} = 0. \tag{16}$$

Substituting eqs. (11)–(14) into eqs. (15) and (16), the governing equations of the FGM-coated half-space can be expressed as

$$\begin{aligned}&(\lambda_i+2\mu_i)\left(\frac{\partial^2 u_i}{\partial r^2}+\frac{1}{r}\frac{\partial u_i}{\partial r}-\frac{1}{r^2}u_i\right)\\&+\frac{\partial\mu_i}{\partial z}\left(\frac{\partial u_i}{\partial z}+\frac{\partial w_i}{\partial r}\right)+\frac{\partial\lambda_i}{\partial r}\left(\frac{u_i}{r}+\frac{\partial w_i}{\partial z}\right)\\&+\mu\frac{\partial^2 u_i}{\partial z^2}+(\lambda_i+\mu_i)\frac{\partial^2 w_i}{\partial r\partial z}+\frac{\partial u_i}{\partial r}\left(\frac{\partial\lambda_i}{\partial r}+2\frac{\partial\mu_i}{\partial r}\right)\\&-3\left(K_i T_i\frac{\partial\alpha_i}{\partial r}+\alpha_i T_i\frac{\partial K_i}{\partial r}+\alpha_i K_i\frac{\partial T_i}{\partial r}\right)=0,\end{aligned} \tag{17}$$

$$\begin{aligned}&\mu_i\left(\frac{\partial^2 w_i}{\partial r^2}+\frac{1}{r}\frac{\partial w_i}{\partial r}\right)+(\lambda_i+\mu_i)\left(\frac{\partial^2 u_i}{\partial r\partial z}+\frac{1}{r}\frac{\partial u_i}{\partial z}\right)\\&+(\lambda_i+2\mu_i)\frac{\partial^2 w_i}{\partial z^2}+\frac{\partial\lambda_i}{\partial z}\left(\frac{u_i}{r}+\frac{\partial u_i}{\partial r}\right)\\&+\left(\frac{\partial\lambda_i}{\partial z}+\frac{2\partial\mu_i}{\partial z}\right)\frac{\partial w_i}{\partial z}+\frac{\partial\mu_i}{\partial r}\left(\frac{\partial u_i}{\partial z}+\frac{\partial w_i}{\partial r}\right)\\&-3\left(K_i T_i\frac{\partial\alpha_i}{\partial r}+\alpha_i T_i\frac{\partial K_i}{\partial r}+\alpha_i K_i\frac{\partial T_i}{\partial r}\right)=0.\end{aligned} \tag{18}$$

The displacements and stresses are continuous at the interface $z = -h$:

$$u_2(r,-h) = u_1(r,-h),\ w_2(r,-h) = w_1(r,-h), \tag{19}$$

$$\sigma_{zz2}(r,-h) = \sigma_{zz1}(r,-h),\ \sigma_{rz2}(r,-h) = \sigma_{rz1}(r,-h). \tag{20}$$

On the surface $z = 0$, the boundary and equilibrium conditions can be stated as follows:

$$\sigma_{zz1} = -p(r),\ \sigma_{rz1} = -fp(r),\ r \leqslant a, \tag{21}$$

$$2\pi\int_0^a p(r)r\,dr = P,\ r \leqslant a. \tag{22}$$

When the temperature dependence of the materials is not considered, the governing equation of thermoelastic contact can be solved using the Hankel transform and singular integral equation technique [31,45,46]. However, considering the temperature-dependent material properties, the thermoelastic contact problem becomes considerably complicated, and it is difficult or even impossible to derive the singular integral equation through integral transformation, which makes the present contact problem analytically intractable. Therefore, the FEM is used to investigate the thermoelastic rotating contact of the FGM-coated half-space with temperature-dependent and arbitrarily varying material properties.

Note that the present model can be easily reduced to the thermoelastic rotating contact of a rigid spherical punch on an FGM-coated half-space without temperature-dependent material properties. Details of the formulation of the reduced model were provided by Liu et al. [45]. In Sect. 5, the theoretical results of the reduced model are used to compare and validate the FEM results of the proposed model. In the reduced model, the material properties of the FGM coating are assumed to vary along the thickness direction according to the exponential form given by eq. (3), except that the Poisson's ratio is assumed to be constant ($v_1(z) = v_m$).

4 Finite element model with temperature-dependency

The FEM model of the thermoelastic rotating contact between a spherical punch and FGM-coated half-space was established using the commercially available finite element software ABAQUS 2019, as shown in Figure 2. The spherical punch is an elastic punch with a large elastic modulus that is approximately 3000 times that of the half-space to mimic a rigid punch. The radius of the spherical punch is 20 mm. The size of the half-space is 200 mm×200 mm×200 mm, which can be considered as a half-space in comparison with the small contact area in the study. The thickness of the FGM coating is h=2 mm.

For the FGM coating, the temperature-dependent and arbitrarily varying material properties are defined using the UMAT and UMATHT subroutines. With the UMAT subroutine, the gradient variation of the elastic modulus, thermal expansion coefficient, and their changes with temperature can be achieved. The UMATHT subroutine can be used to model the gradient variation of the thermal conductivity and its temperature dependency. After fixing the coordinate

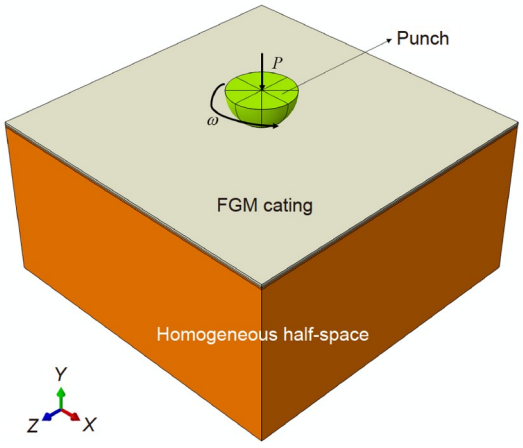

Figure 2 (Color online) FEM contact model of spherical punch and FGM-coated half-space with temperature-dependent material properties.

system, the thermoelastic parameters of the FGM coating are related to the original coordinates at each material point. Therefore, the initial coordinates of the material points are extracted to ensure that the thermoelastic parameters of the FGM coating are calculated using the original coordinates during the calculation process. This process is as follows.

(1) In the first step and the first increment of the calculation, the original coordinates of all material points in the FGM coating are saved through the state variable STATEV in the UMAT and UMATHT subroutines.

(2) The state variable STATEV and temperature are fetched to calculate the thermoelastic parameters at all material points.

(3) The elastic stress-strain relationship is provided in the UMAT subroutine to update the stress and strain.

A steady-state thermomechanical coupled analysis is conducted to solve the thermoelastic rotating contact problem. The contact between the punch and FGM-coated half-space is defined by using a master-slave algorithm. The punch surface is the contact master surface and the top surface of the elastic half-space is the contact slave surface. The sliding formulation is set as finite sliding, and the discretization is conducted using the surface-to-surface method. The penalty function method is used to define the Coulomb friction. In steady-state thermomechanical coupling analysis, the frictional heat on the contact region is defined using the FRIC subroutine. In this subroutine, the incremental friction dissipation is used to represent the frictional heat, which is calculated as the product of the frictional stress and slip increment. Moreover, in the contact-property option, we set the fraction of the frictional heat distribution to the slave surface to 100%, which means that all the heat is transferred into the FGM-coated half-space.

In this analysis, 4-node linear, 6-node linear, and 8-node trilinear displacement and temperature elements (C3D4T, C3D6T, and C3D8T, respectively) are used. The total number of elements in this model is 240498, which can achieve convergent results. The numbers of C3D8T, C3D6T, and C3D8T elements are 226525, 3056, and 10917, respectively. As shown in Figure 3, the meshes near the contact region are sufficiently refined to ensure the accuracy of the results.

A concentrated normal load P and angular velocity ω are applied to the reference point of the punch. The punch displacements in the x and z directions are fixed. Therefore, the punch can move in the y direction and rotate around the y direction under loading. The bottom surface of the elastic half-space is fixed, and the initial temperature boundary condition $T=T_0$ is imposed on the sides and bottom of the half-space.

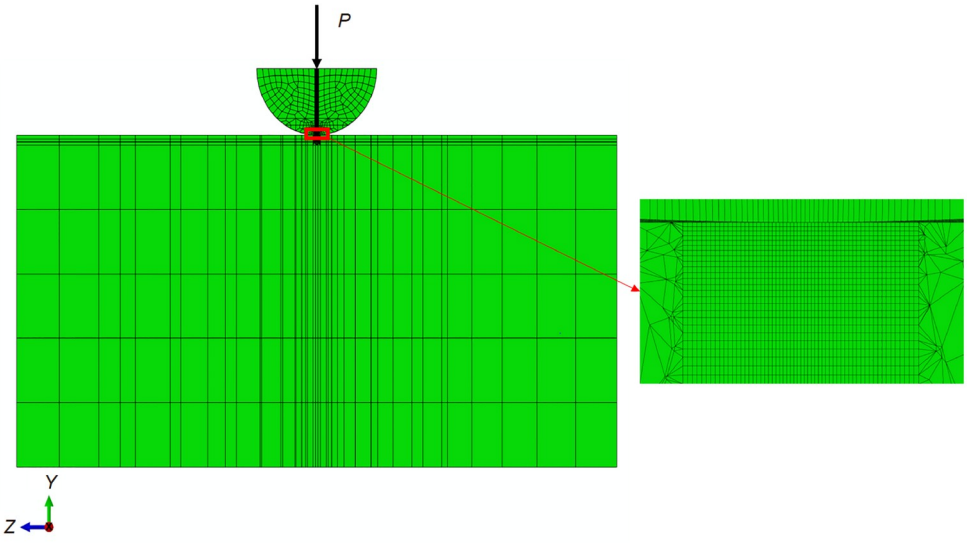

Figure 3 (Color online) Total meshes and locally fine meshes in the contact region.

5 Results and discussion

In this section, the thermoelastic rotating contact of a rigid spherical punch and an FGM-coated half-space with temperature-dependent and arbitrarily varying material properties are studied using FEM. The upper layer material of the coating is ceramic, whereas the lower layer material is metal. Two coating systems are considered in the analysis: Si_3N_4-Al6061 and ZrO_2-Al6061. The temperature-dependent parameters of these materials are listed in Table 1 [44,47,48]. As shown in Sects. 5.2–5.4, the variations in the thermoelastic properties follow the power-law form, i.e., case I. In Sect. 5, we discuss the effects of the different gradient forms. Unless otherwise stated, the following parameters are adopted: gradient index $n = 2$, angular velocity $\omega = 140$ rad/s, friction coefficient $f = 0.3$, initial temperature $T_0 = 300$ K and coating thickness $h = 2$ mm.

5.1 Comparison study

The contact problem between a spherical punch and a homogeneous Al6061 half-space is computed using ABAQUS 2019. The material parameters at room temperature (T_0=300 K) are used with the elastic modulus and Poisson's ratio of E=116 GPa and ν=0.333, respectively. A concentrated normal load P=200 N is applied to the punch. Figure 4 shows the comparison between the FEM and theoretical results of the contact pressure. These results agree well with Johnson's results [49].

By neglecting the frictional heat and temperature dependence, the present model can be reduced to the contact between a spherical punch and an FGM-coated half-space. The upper layer material of the coating is ZrO_2 and the lower layer material and substrate are Al6061. The gradient form obeys an exponential form. The elastic moduli and Poisson's ratios of ZrO_2 and Al6061 are listed in Table 1 with T=300 K. The Poisson's ratio of the FGM coating is assumed to be constant, i.e., $\nu_1(z)=\nu_0$. Figure 5 shows the FEM results and Liu and Wang's results with h=2 mm. We can observe that the present results are very close to those of Liu and Wang [50].

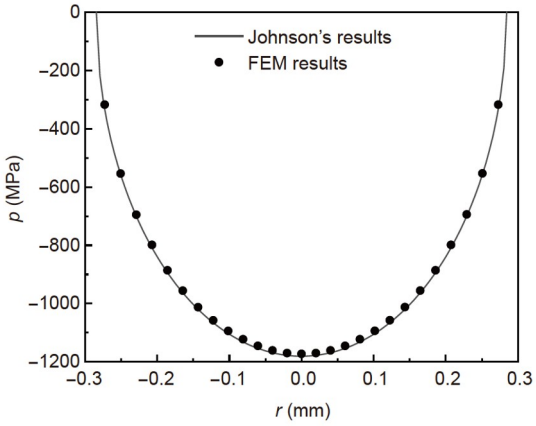

Figure 4 Comparison of the contact pressure between the present FEM results and Johnson's results.

The theoretical solutions of the thermoelastic rotating contact of the FGM-coated half-space without considering the temperature dependence were provided by Liu et al. [45]. The material properties of the ZrO_2-Al6061 FGM coating follow an exponential form. The material parameters of ZrO_2 and Al6061 are listed in Table 1 at T=300 K. The Poisson's ratio of the FGM coating is assumed to be constant, i.e., $\nu_1(z)=\nu_0$. The proposed FEM model can be easily modified for this case. Figure 6 shows a comparison between the FEM and theoretical results of the contact pressure and temperature with h=2 mm and ω = 6 rad/s. Both results are in good agreement.

Table 1 Temperature-dependent parameters of the elastic modulus E (GPa), Poisson's ratio ν, thermal expansion coefficient α (1/K), and thermal conductivity k (W/(m K))

	Material	B_{-1}	B_0	B_1	B_2	B_3
E	Si_3N_4	0	348.43	-3.070×10^{-4}	2.160×10^{-7}	-8.946×10^{-11}
	ZrO_2	0	132.20	-3.805×10^{-4}	-6.127×10^{-8}	0
	Al6061	0	81.62	-3.7785×10^{-4}	3.1365×10^{-8}	-2.8103×10^{-10}
ν	Si_3N_4	0	0.2400	0	0	0
	ZrO_2	0	0.3330	0	0	0
	Al6061	0	0.2349	0.0025	-4.688×10^{-6}	3.113×10^{-9}
α	Si_3N_4	0	5.8723×10^{-6}	9.095×10^{-6}	0	0
	ZrO_2	0	13.300×10^{-6}	-1.421×10^{-3}	9.549×10^{-7}	0
	Al6061	0	1.0062×10^{-6}	0.0562	-9.214×10^{-6}	-5.267×10^{-10}
k	Si_3N_4	0	9.19	0	0	0
	ZrO_2	0	1.78	0	0	0
	Al6061	0	458.1	-3.328×10^{-3}	6.236×10^{-6}	-3.747×10^{-9}

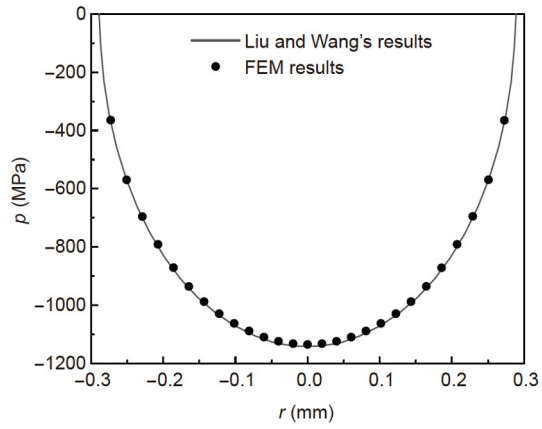

Figure 5 Comparison of the contact pressure between the FEM results and Liu and Wang's results with h=2 mm [50].

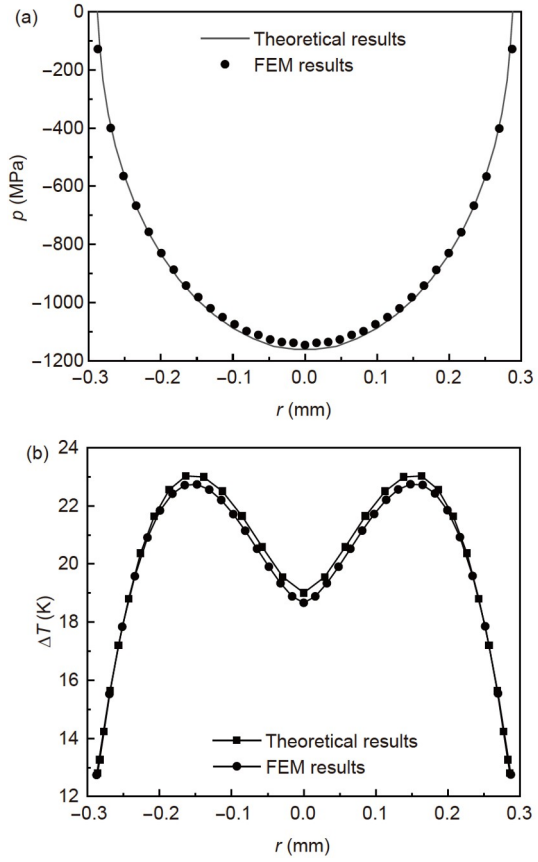

Figure 6 Comparison of FEM results and theoretical results of the thermoelastic rotating contact without considering the temperature dependence with h=2 mm and ω = 6 rad/s. (a) Contact pressure; (b) temperature.

5.2 Effect of temperature dependence

Figure 7 shows the effect of temperature dependence on the contact pressure p, temperature T, and in-plane stress σ_{rr} of the Si_3N_4-Al6061 FGM coating structure. We can observe that the temperature dependence has almost no effect on the contact pressure, temperature, and in-plane stress. This is

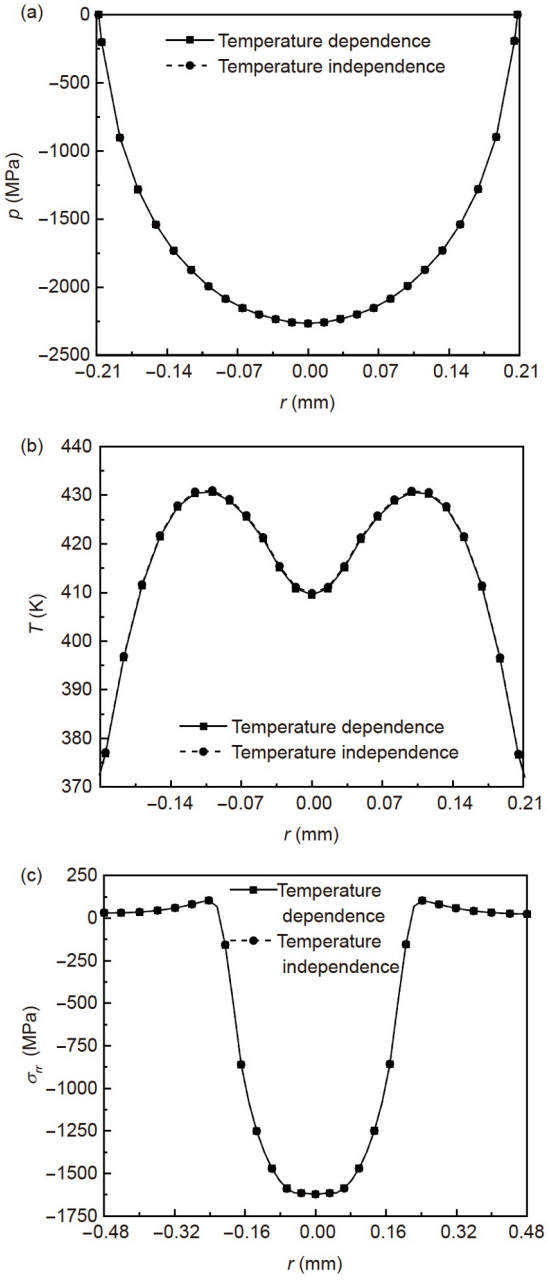

Figure 7 Effect of temperature dependence on the thermoelastic contact behavior of the Si_3N_4-Al6061 FGM coating structure (case I) with n = 2, ω = 140 rad/s and f = 0.3. (a) Contact pressure; (b) temperature; (c) in-plane stress.

because the upper layer material of the coating is Si_3N_4 ceramic, which is insensitive to temperature changes. Interestingly, the temperature field of the spherical punch has an M-shaped distribution. This is attributed to the fact that the heat flux density is zero at the contact center r = 0, resulting in a temperature at the contact center lower than that at other positions. We observed that tensile stresses occurred at the edge of the contact area.

Figure 8 exhibits the effect of the temperature dependence on the contact pressure p, temperature T, and in-plane stress σ_{rr} of the ZrO_2-Al6061 FGM coating structure. Because the

Si_3N_4 ceramic is sensitive to temperature changes, the results of the contact pressure, temperature, and in-plane stress accounting for the temperature dependence are smaller than those with temperature independence near the center of the contact area. Owing to the temperature increaing, the tensile stress does not appear at the edges of the contact area. Thus, the M-shaped temperature distribution affects the in-plane stress σ_{rr} near the contact center.

According to the results in Figures 7 and 8, it can be concluded that the ZrO_2-Al6061 system is more sensitive to temperature dependence compared with the Si_3N_4-Al6061 system. The ZrO_2-Al6061 system produces a higher temperature field under the same conditions. Therefore, only the results of the ZrO_2-Al6061 system are discussed further in the subsequent examples.

5.3 Effect of gradient index *n*

Figure 9 illustrates the effect of the gradient index n on the contact pressure p, temperature T, and in-plane stress σ_{rr} of

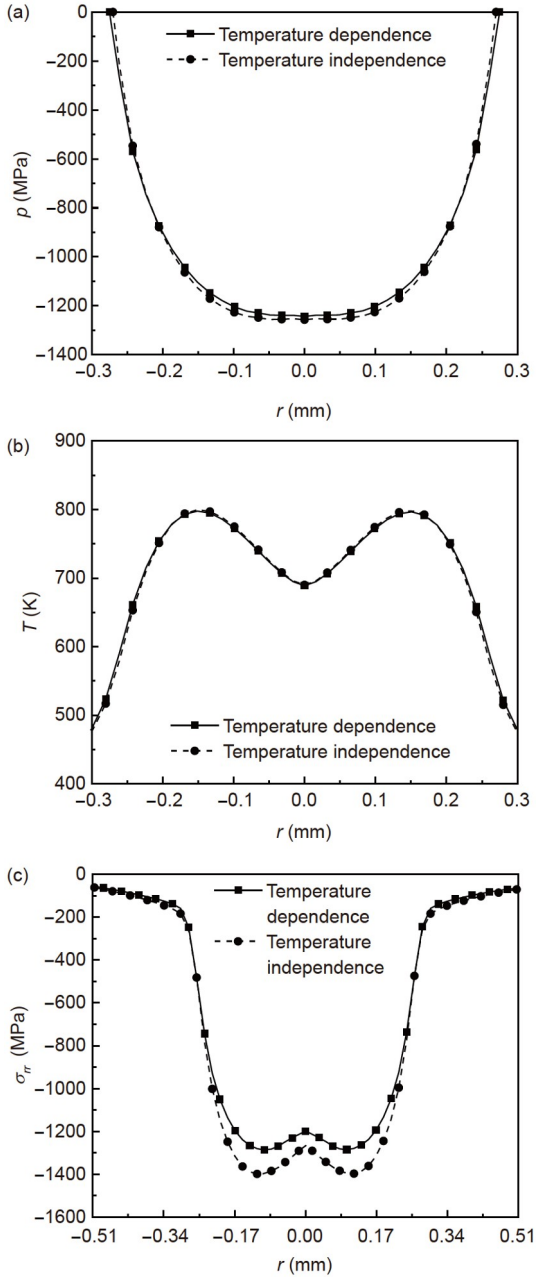

Figure 8 Effect of the temperature dependence on the thermoelastic contact behavior of the ZrO_2-Al6061 FGM coating structure (case I) with n = 2, ω = 140 rad/s and f = 0.3. (a) Contact pressure; (b) temperature; (c) in-plane stress.

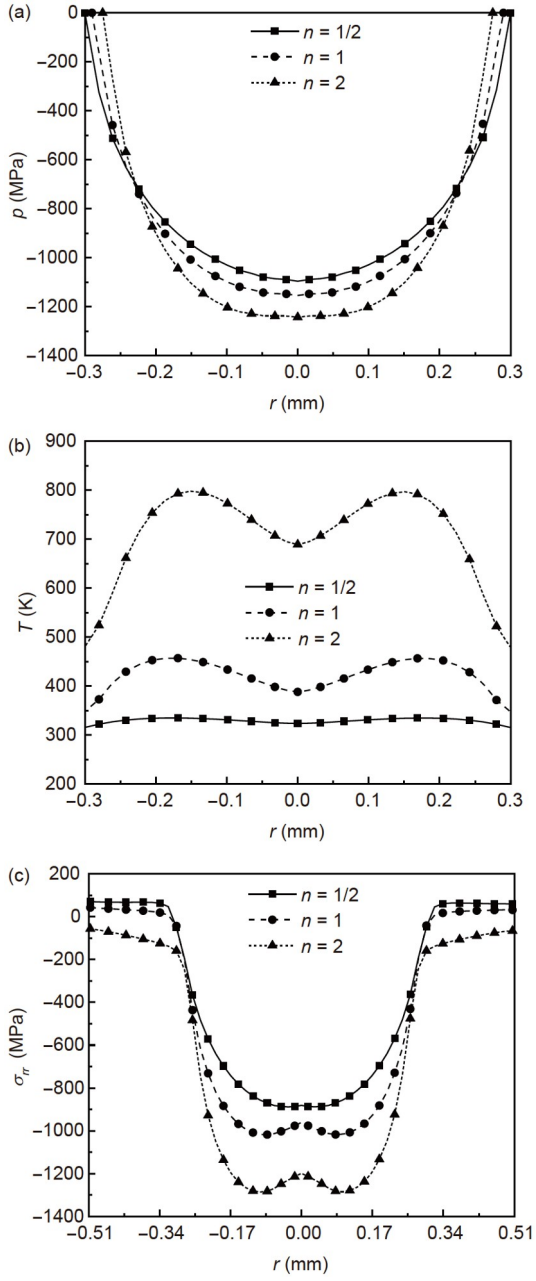

Figure 9 Effect of the gradient index on the thermoelastic contact behavior of the ZrO_2-Al6061 FGM coating structure (case I) with ω = 140 rad/s and f = 0.3. (a) Contact pressure; (b) temperature; (c) in-plane stress.

the ZrO_2-Al6061 FGM coating structure. Clearly, the gradient index n has a significant influence on the contact pressure, temperature, and in-plane stress. With the increase of n, the maximum values of the contact pressure, temperature, and in-plane stress increase. Regarding the in-plane stress, it is observed that the tensile stresses occur at the edge of the contact region during n=1/2 and n=1. This tensile stress is the main reason for the surface crack initiation and contact damage at the contact surface. However, the tensile stress changes to the compressive stress when n increases to 2. These results imply that thermoelastic rotating contact damage can be effectively improved by adjusting the gradient index.

5.4 Effect of friction coefficient f and angular velocity ω

Figure 10 shows the effect of the friction coefficient on the contact pressure p, temperature T, and in-plane stress σ_{rr} of the ZrO_2-Al6061 FGM coating structure. With the increase of f, the maximum values of the contact pressure, temperature, and in-plane stress clearly increase. For the in-plane stress, it can be observed that the tensile stresses occur at the edge of the contact region when f = 0 and f = 0.1. However, when f increases to 0.2 or 0.3, the frictional heat increases, and the tensile stress changes to compressive stress. This is because the frictional heat contributes to the compression of the in-plane stress, and therefore, can alleviate the tensile stress. Shi [51] observed a similar phenomenon when he studied the thermal contact of multi-layered elastic solids.

Figure 11 depicts the effect of angular velocity on the contact pressure p, temperature T, and in-plane stress σ_{rr} of the ZrO_2-Al6061 FGM coating structure. With the increase of ω, the maximum values of the contact pressure, temperature, and in-plane stress increase markedly. For the in-plane stress, the tensile stresses occur at the edge of the contact area when ω=40 rad/s. However, the tensile stress changes to compressive stress when ω increases to 90 rad/s or 140 rad/s. This is because a high angular velocity produces a large amount of frictional heat, which in turn results in a decrease in the tensile stress.

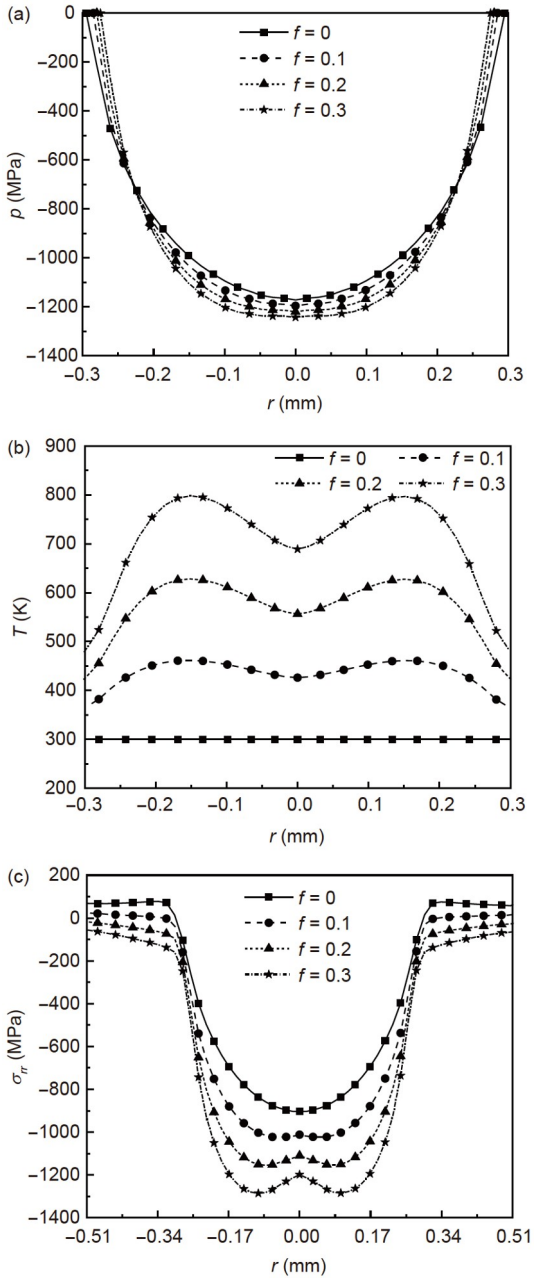

Figure 10 Effect of the friction coefficient on the thermoelastic contact behavior of the ZrO_2-Al6061 FGM coating structure (case I) with n = 2 and ω = 140 rad/s. (a) Contact pressure; (b) temperature; (c) in-plane stress.

5.5 Effect of different gradient forms

Figure 12 presents the effects of the different gradient forms on the contact pressure p, temperature T, and in-plane stress σ_{rr} of the ZrO_2-Al6061 FGM coating structure. The power-law form (case I), exponential form (case II), cosine form (case III), and sinusoidal form (case IV) are considered in this example. Eqs. (2)–(5) describe the expressions for the four cases. In case I, we set the gradient index as n=3. Among the four cases, the sinusoidal form has the smallest contact pressure, temperature, and in-plane stress, whereas the power-law form has the largest. Clearly, the in-plane stress at the edge is tensile in case IV, whereas it becomes compressive in the other three cases. Therefore, it is concluded that the tensile stress can also reverse to the compressive stress by varying the gradient form.

The present contact model considers that the material properties of the FGM coating vary arbitrarily along the thickness direction. Therefore, it is convenient for analyzing the effects of the gradient index and gradient form on the thermoelastic contact behavior of FGM coatings. The above results imply that the tensile stress can undergo stress reversal and become compressive stress by varying the gra-

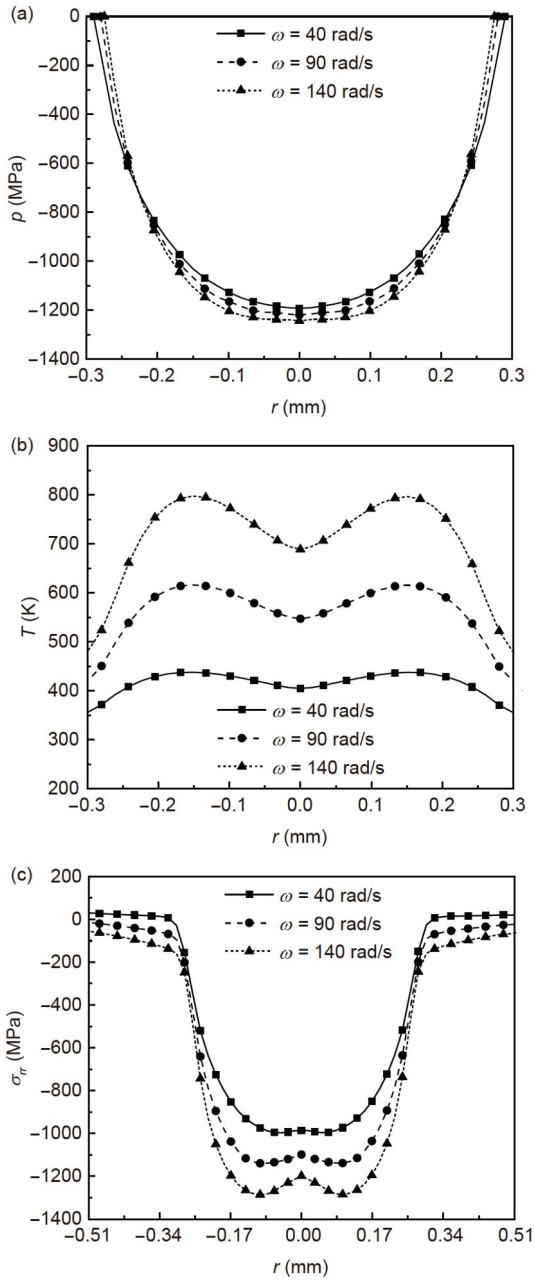

Figure 11 Effect of the angular velocity on the thermoelastic contact behavior of the ZrO_2-Al6061 FGM coating structure (case I) with $n = 2$ and $f = 0.3$. (a) Contact pressure; (b) temperature; (c) in-plane stress.

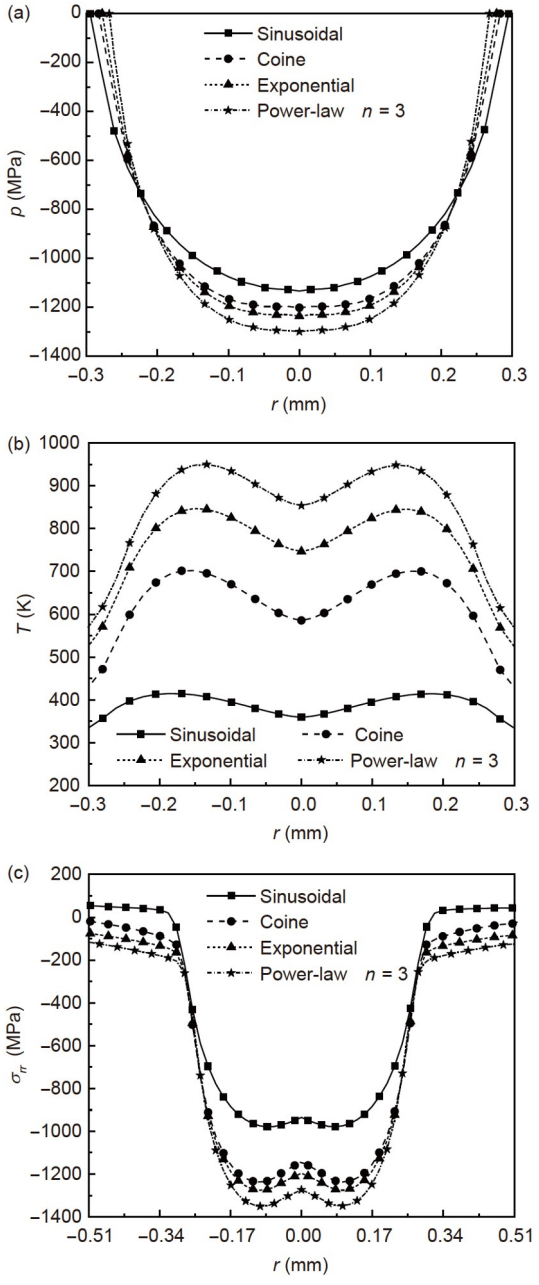

Figure 12 Effect of the gradient form on the thermoelastic contact behavior of the ZrO_2-Al6061 FGM coating structure with $\omega = 140$ rad/s and $f = 0.3$. (a) Contact pressure; (b) temperature field; (c) in-plane stress.

dient index and gradient form. Consequently, the thermoelastic rotating contact damage can be minimized by adjusting the gradient index and gradient form. This paper provides coating design strategies to resist thermoelastic contact damage.

6 Conclusions

In this paper, the thermoelastic rotating contact of a spherical punch on an FGM-coated half-space with arbitrary material properties is investigated. The material parameters are temperature-dependent. The effects of the temperature dependence, gradient index, friction coefficient, angular velocity, and gradient form are discussed. The main conclusions of this study are summarized as follows.

(1) The temperature field of the spherical punch exhibits an M-shaped distribution because the heat flux density is zero at the contact center.

(2) When the upper layer material of the coating is sensitive to the temperature changes, the temperature dependence may have a relatively significant effect on the thermoelastic

contact behaviors.

(3) Increasing the gradient index, friction coefficient, and angular velocity results in a significant increase in the maximum values of the contact pressure, temperature, and in-plane stress.

(4) The tensile stress can undergo stress reversal and become compressive stress by varying the gradient index and gradient form. This indicates that thermoelastic contact damage can be minimized by adjusting the gradient index and gradient form.

(5) The frictional heat contributes to the compression of the in-plane stress and can therefore alleviate the tensile stress.

This work was supported by the National Natural Science Foundation of China (Grant Nos. 11725207 and 12021002).

1 Barber J R, Ciavarella M. Contact mechanics. Int J Solids Struct, 2000, 37: 29–43
2 Suresh S. Graded materials for resistance to contact deformation and damage. Science, 2001, 292: 2447–2451
3 Zhang Y, Kim J W. Graded zirconia glass for resistance to veneer fracture. J Dent Res, 2010, 89: 1057–1062
4 Jørgensen O, Giannakopoulos A E, Suresh S. Spherical indentation of composite laminates with controlled gradients in elastic anisotropy. Int J Solids Struct, 1998, 35: 5097–5113
5 Suresh S, Olsson M, Giannakopoulos A E, et al. Engineering the resistance to sliding-contact damage through controlled gradients in elastic properties at contact surfaces. Acta Mater, 1999, 47: 3915–3926
6 Pender D C, Padture N P, Giannakopoulos A E, et al. Gradients in elastic modulus for improved contact-damage resistance. Part I: The silicon nitride–oxynitride glass system. Acta Mater, 2001, 49: 3255–3262
7 Pender D C, Thompson S C, Padture N P, et al. Gradients in elastic modulus for improved contact-damage resistance. Part II: The silicon nitride-silicon carbide system. Acta Mater, 2001, 49: 3263–3268
8 Kashtalyan M, Menshykova M. Three-dimensional elastic deformation of a functionally graded coating/substrate system. Int J Solids Struct, 2007, 44: 5272–5288
9 Chen P J, Chen S H. Partial slip contact between a rigid punch with an arbitrary tip-shape and an elastic graded solid with a finite thickness. Mech Mater, 2013, 59: 24–35
10 Demirhan N, Kanber B. Finite element analysis of frictional contacts of FGM coated elastic members. Mech Based Des Struct Machines, 2013, 41: 383–398
11 Jobin K J, Abhilash M N, Murthy H. A simplified analysis of 2D sliding frictional contact between rigid indenters and FGM coated substrates. Tribol Int, 2017, 108: 174–185
12 Yilmaz K B, Comez I, Yildirim B, et al. Frictional receding contact problem for a graded bilayer system indented by a rigid punch. Int J Mech Sci, 2018, 141: 127–142
13 Chen X W, Yue Z Q. Contact mechanics of two elastic spheres reinforced by functionally graded materials (FGM) thin coatings. Eng Anal Bound Elem, 2019, 109: 57–69
14 Alinia Y, Asiaee A, Hosseini-nasab M. Stress analysis in rolling contact problem of a finite thickness FGM layer. Meccanica, 2018, 54: 183–203
15 Çömez I, El-Borgi S, Yildirim B. Frictional receding contact problem of a functionally graded layer resting on a homogeneous coated half-plane. Arch Appl Mech, 2020, 90: 2113–2131
16 Guler M A, Erdogan F. Contact mechanics of graded coatings. Int J Solids Struct, 2004, 41: 3865–3889
17 Guler M A, Erdogan F. The frictional sliding contact problems of rigid parabolic and cylindrical stamps on graded coatings. Int J Mech Sci, 2007, 49: 161–182
18 Ke L L, Wang Y S. Two-dimensional sliding frictional contact of functionally graded materials. Eur J Mech-A Solids, 2007, 26: 171–188
19 Liu T J, Wang Y S, Zhang C Z. Axisymmetric frictionless contact of functionally graded materials. Arch Appl Mech, 2008, 78: 267–282
20 Dag S, Guler M A, Yildirim B, et al. Sliding frictional contact between a rigid punch and a laterally graded elastic medium. Int J Solids Struct, 2009, 46: 4038–4053
21 Çömez İ. Contact problem for a functionally graded layer indented by a moving punch. Int J Mech Sci, 2015, 100: 339–344
22 Chen P J, Chen S H, Peng J. Frictional contact of a rigid punch on an arbitrarily oriented gradient half-plane. Acta Mech, 2015, 226: 4207–4221
23 Chen P J, Chen S H, Peng J. Sliding contact between a cylindrical punch and a graded half-plane with an arbitrary gradient direction. J Appl Mech, 2015, 82: 041008
24 El-Borgi S, Abdelmoula R, Keer L. A receding contact plane problem between a functionally graded layer and a homogeneous substrate. Int J Solids Struct, 2006, 43: 658–674
25 El-Borgi S, Usman S, Güler M A. A frictional receding contact plane problem between a functionally graded layer and a homogeneous substrate. Int J Solids Struct, 2014, 51: 4462–4476
26 Aizikovich S M, Krenev L I, Trubchik I S. The deformation of a half-space with a gradient elastic coating under arbitrary axisymmetric loading. J Appl Math Mech, 2008, 72: 461–467
27 Aizikovich S M, Alexandrov V M, Kalker J J, et al. Analytical solution of the spherical indentation problem for a half-space with gradients with the depth elastic properties. Int J Solids Struct, 2002, 39: 2745–2772
28 Barik S P, Kanoria M, Chaudhuri P K. Steady state thermoelastic contact problem in a functionally graded material. Int J Eng Sci, 2008, 46: 775–789
29 Shahzamanian M M, Sahari B B, Bayat M, et al. Transient and thermal contact analysis for the elastic behavior of functionally graded brake disks due to mechanical and thermal loads. Mater Des, 2010, 31: 4655–4665
30 Afsar A M, Go J. Finite element analysis of thermoelastic field in a rotating FGM circular disk. Appl Math Model, 2010, 34: 3309–3320
31 Liu J, Ke L L, Wang Y S. Two-dimensional thermoelastic contact problem of functionally graded materials involving frictional heating. Int J Solids Struct, 2011, 48: 2536–2548
32 Krenev L I, Aizikovich S M, Tokovyy Y V, et al. Axisymmetric problem on the indentation of a hot circular punch into an arbitrarily nonhomogeneous half-space. Int J Solids Struct, 2015, 59: 18–28
33 Kulchytsky-Zhyhailo R, Bajkowski A S. Axisymmetrical problem of thermoelasticity for halfspace with gradient coating. Int J Mech Sci, 2016, 106: 62–71
34 Zhang H B, Wang W Z, Zhang S G, et al. Semi-analytical solution of three-dimensional steady state thermoelastic contact problem of multilayered material under friction heating. Int J Thermal Sci, 2018, 127: 384–399
35 Çömez İ. Thermoelastic receding contact problem of a layer resting on a half plane with frictional heat generation. J Thermal Stresses, 2021, 44: 566–581
36 Choi H J, Paulino G H. Thermoelastic contact mechanics for a flat punch sliding over a graded coating/substrate system with frictional heat generation. J Mech Phys Solids, 2008, 56: 1673–1692
37 Barik S P, Chaudhuri P K. Thermoelastic contact between a functionally graded elastic cylindrical punch and a half-space involving frictional heating. J Eng Math, 2012, 76: 123–138
38 Chen P J, Chen S H, Peng Z L. Thermo-contact mechanics of a rigid cylindrical punch sliding on a finite graded layer. Acta Mech, 2012,

223: 2647–2665
39 Chen P J, Chen S H. Thermo-mechanical contact behavior of a finite graded layer under a sliding punch with heat generation. Int J Solids Struct, 2013, 50: 1108–1119
40 Liu J, Ke L L, Wang Y S, et al. Thermoelastic frictional contact of functionally graded materials with arbitrarily varying properties. Int J Mech Sci, 2012, 63: 86–98
41 Balci M N, Dag S, Yildirim B. Subsurface stresses in graded coatings subjected to frictional contact with heat generation. J Thermal Stresses, 2017, 40: 517–534
42 Nili A, Adibnazari S, Karimzadeh A. Stress field in the thermoelastic rolling contact of graded coatings. Arch Appl Mech, 2018, 88: 1805–1814
43 Nili A, Adibnazari S, Karimzadeh A. Rolling contact mechanics of graded coatings involving frictional heating. Acta Mech, 2019, 230: 1981–1997
44 Kim Y W. Temperature dependent vibration analysis of functionally graded rectangular plates. J Sound Vib, 2005, 284: 531–549
45 Liu J, Ke L L, Zhang C Z. Axisymmetric thermoelastic contact of an FGM-coated half-space under a rotating punch. Acta Mech, 2021, 232: 2361–2378
46 Civelek M B. The axisymmetric contact problem for an elastic layer on a frictionless half-space. Dissertation for Doctoral Degree. Bethlehem: Lehigh University, 1972
47 Malekzadeh P, Ghorbani Shenas A, Ziaee S. Thermal buckling of functionally graded triangular microplates. J Braz Soc Mech Sci Eng, 2018, 40: 418
48 Gao J X, Cao Y Z, Lu L H, et al. Study on the interaction between nanosecond laser and 6061 aluminum alloy considering temperature dependence. J Alloys Compd, 2022, 892: 162044
49 Johnson K L. Contact Mechanics. Cambridge: Cambridge University Press, 1985
50 Liu T J, Wang Y S. Axisymmetric frictionless contact problem of a functionally graded coating with exponentially varying modulus. Acta Mech, 2008, 199: 151–165
51 Shi Z. Mechanical and thermal contact analysis in layered elastic solids. Dissertation for Doctoral Degree. Minnesota: University of Minnesota, 2001